

# A Centrifugal Model Test on Seismic Reinforcement for Embankments on Peaty Ground

**Shin'ichi Kajitori, Satoshi Nishimoto, Hirochika Hayashi, Hijiri Hashimoto**  
*Civil Engineering Research Institute for Cold Region (CERI)*



## SUMMARY

In Japan's northernmost region of Hokkaido, the Great East Japan Earthquake of 2011 and other large-scale tremors have caused severe liquefaction damage to river embankments in addition to influencing their foundation ground as predicted.

The peaty ground distributed extensively across cold regions of Japan is highly organic and extremely soft. As consolidation settlement is significant and liquefied layers are deeper in embankments on such ground, more extensive damage may occur to structures supported by it. Against this background, a dynamic centrifuge model test was conducted to investigate liquefaction countermeasures for such embankments. The results of the experiment, which was conducted for existing embankments, revealed that the dissipation of excess pore water pressure can be facilitated in liquefied layers at the bottom of embankments, and that settlement can be controlled using gabion boxes.

*Keywords: centrifugal model test, peaty ground, lateral flow, excess pore water pressure, gabion box*

## 1. INTRODUCTION

Japan is located in the circum-Pacific orogenic belt, and is affected by frequent earthquakes and volcanic eruptions. The country's terrain is characterized by steep landforms and topographic and geological conditions that bring a high likelihood of natural disasters due to heavy and frequent rainfall. In the magnitude-9.0 Great East Japan Earthquake of March 2011, river embankments were severely damaged as a result of liquefaction (Photo 1)<sup>1)</sup>. This phenomenon was expected in the foundation ground of embankments, but the earthquake caused unexpected liquefaction of embankments themselves, and many such structures sustained severe damage.

Highly organic and extremely compressible peaty ground with unique properties is found extensively across Japan's northernmost region of Hokkaido. In several large earthquakes that have hit the area in the past, considerable deformation has been seen in road and river embankments built on such ground (Photo 2)<sup>2)</sup>. With this in mind, CERI conducted analysis of the mechanism behind such damage and succeeded in reproducing deformation modes characteristic to embankments on peaty ground via a dynamic centrifuge model test<sup>3)</sup>.

As no rational methods for seismic reinforcement have yet been established, the test was designed to investigate such approaches for existing embankments on peaty ground.



Photo 1. Liquefaction damage caused by the Great East Japan Earthquake of 2011 (river embankment)



Photo 2. Liquefaction damaged caused by the Kushiro-oki Earthquake of 1993 (river embankment)

## 2. MECHANISM BEHIND DAMAGE TO EMBANKMENTS ON PEATY GROUND AND DISCUSSION OF SPECIFIC DAMAGE CASES

### 2.1. Mechanism behind embankment damage

Embankments built on soft ground undergo sinking in response to consolidation settlement, and their bases become concave (Fig. 1). It is assumed that density and restraining force at the bottom of an embankment decreases in this consolidation settlement process, and that the section where embankment material sinks into soft ground (i.e., the settled embankment layer) becomes saturated below the groundwater level. For embankments made of sandy soil, earthquake-related liquefaction of this section is presumed to result in loss of shear strength and significant deformation.

As peaty ground is highly compressible, the settlement of embankments built on such land is significant. This gives rise to concerns over deepening of the settled embankment layer and even more serious damage from liquefaction.

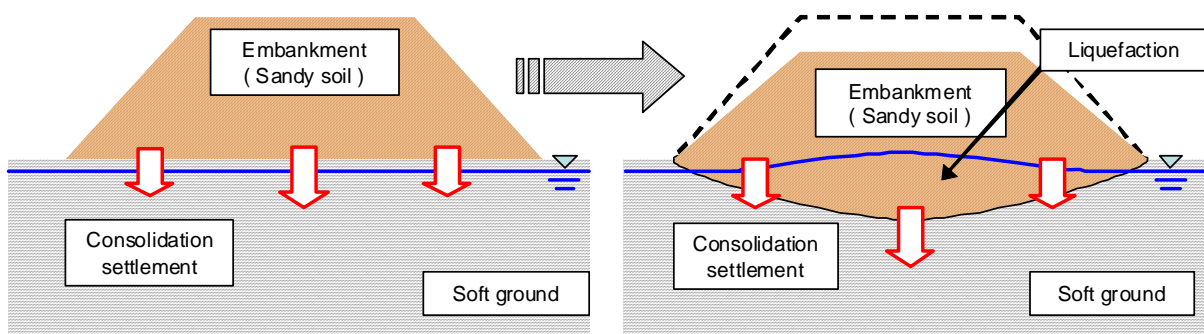


Fig. 1. Left: Consolidation settlement occurs gradually in embankments built on soft ground.

Right: Consolidation settlement progresses with time and forms a saturated section in the embankment.

### 2.2. Damage in the Kushiro-oki Earthquake of 1993

The Hokkaido Kushiro-oki Earthquake of 1993 caused significant deformation of an embankment along the Tokachi River (Photo 2). The crown and the top of the fore land-side slope settled by 2 to 3.5 m, and large cracking affected the embankment body. A post-disaster survey revealed that, although the surface layer of the foundation was peaty ground unaffected by liquefaction, traces of sand boils were found near the crown.

Studies by CERI<sup>2)</sup> and Sasaki<sup>4)</sup> assumed that these traces resulted from liquefaction of the saturated section at the bottom of the embankment. As peat is extremely compressible, it undergoes significant settlement, and places where peat accumulates into layers often have high groundwater levels close to the surface. In this case, it is presumed that the embankment material sank into the peaty ground and became saturated below the groundwater level, and that this saturated section became liquefied in the earthquake. A ground survey performed after the disaster confirmed the presence of embankment material below the groundwater level.

### 3. CENTRIFUGE MODEL TEST OVERVIEW

#### 3.1. Experiment objective and countermeasure selection

In this study, a centrifuge model test was conducted with various levels of acceleration to determine the resulting degree of damage to embankments on peaty ground. For each level, embankment settlement and excess pore water pressure in the settled layers were measured.

An experiment with two levels of acceleration was also conducted to examine the effects of gabion box-related countermeasures selected based on existing embankments. Countermeasures involving large-scale ground improvement are not realistic for reinforcing existing embankments, and cost-effective approaches are also required due to the significant length of road and river embankments. Accordingly, a method involving the placement of gabion boxes at the toe of the slope was selected because the approach is expected to provide drainage and embankment restraint effects, and because such boxes are easy to install at low cost due to their widespread use in civil engineering work.

The model was built at a scale of 1:50, and the excitation test was conducted in a centrifuge field of 50 G (G = gravitational acceleration).

#### 3.2. Experiment conditions (embankment preparation and excitation)

Table 1 lists the details of the experiment cases. Cases 1 to 5 were without countermeasures, and the cross section of the model for these cases is shown in Fig. 2. Cases 6 and 7 were with countermeasures using gabion boxes, and the cross section of the model for these cases is shown in Fig. 3. The inputs were 20 sine waves with a frequency of 2 Hz and a period of 0.5 seconds (model: 100 Hz and 0.01 sec.). The experiment conditions other than the input acceleration were the same for all cases. The input acceleration values are shown in Table 1.

The foundation ground (peat), embankment material and shape were the same in all cases. Table 2 shows the embankment construction conditions (degree of compaction, embankment height, crown width and settled embankment layer thickness).

In all cases, the model was fitted with a laser displacement gauge and a pore water pressure meter.

Table 1. Experiment cases

Case	Input acceleration	Countermeasures
1	65 m/s <sup>2</sup> (equivalent to 130 gal)	None
2	175 m/s <sup>2</sup> (equivalent to 350 gal)	
3	275 m/s <sup>2</sup> (equivalent to 550 gal)	
4	325 m/s <sup>2</sup> (equivalent to 650 gal)	
5	350 m/s <sup>2</sup> (equivalent to 700 gal)	
6	175 m/s <sup>2</sup> (equivalent to 350 gal)	Installation of gabion boxes
7	275 m/s <sup>2</sup> (equivalent to 550 gal)	

Numbers in parentheses represent full-scale values.

Table 2. Embankment shape/construction conditions (uniform for all cases)

Degree of compaction	Embankment height	Embankment crown	Thickness of sunken embankment layer
85%	5 m	5 m	2 m

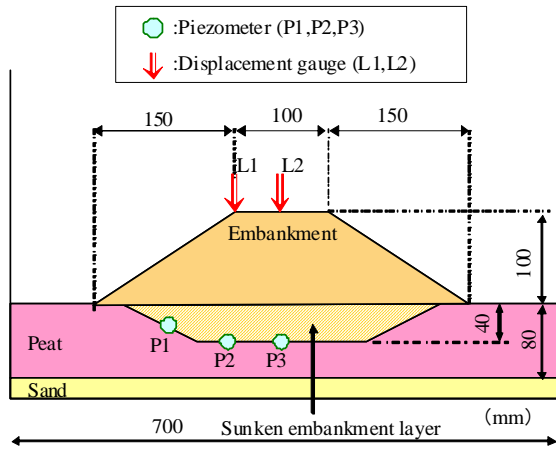


Fig. 2. Cross section of the model without countermeasures (Cases 1 – 4)

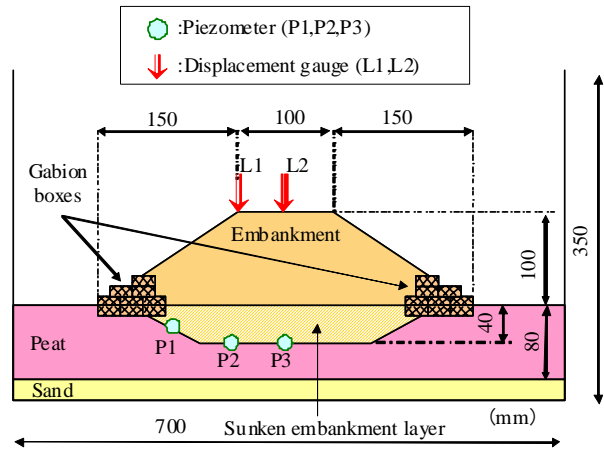


Fig. 3. Cross section of the model with countermeasures using gabion boxes (Cases 5 and 6)

### 3.3. Experiment procedure

Figure 4 shows the experiment procedure. Specifically, a 2-cm sand layer with a relative density of  $D_r = 90\%$  was first created using the air pluviation method to provide drainage at the bottom of the peat layer, and was saturated by supplying water through porous stone. Next, peat prepared by mixing horticultural peat moss and kaolin clay in equal amounts and adjusting the initial water content to 600% was poured in gradually. Horticultural peat moss was dried at  $60^\circ\text{C}$  and broken into pieces measuring 0.85 mm or smaller before mixing (see Table 3 for its main physical properties). Self-weight consolidation of the peaty layer was then performed in a centrifuge field (50 G).

After the foundation ground had been formed as described above, a settled embankment layer (i.e., a liquefied layer) was made. Peaty ground was excavated to form a given shape, and Toyoura sand was poured into the hole at a relative density of  $D_r = 35\%$  using the air pluviation method. Considering that the density and restraining force of actual embankments are reduced in the compaction process, conditions under which liquefaction was likely were set for the settled embankment layer to make liquefaction damage more prominent. To this end, Toyoura sand was used for the settled embankment layer to give a relative density of  $D_r = 35\%$ .

After the settled embankment layer was complete, the embankment was built. Its material was made by mixing Toyoura sand and kaolin clay at a dry-weight ratio of 8 to 2 and adjusting it to the optimum moisture content. Table 4 lists the major physical properties of the embankment material.

After the completion of the model, the soil layer was placed on the centrifuge. Silicon oil with a dynamic viscosity 50 times as high as that of water was supplied to the settled embankment layer to saturate it. Completion of the silicon oil supply was verified using the pore water pressure meter, a camera was placed next to the earth tank, and excitation was performed.

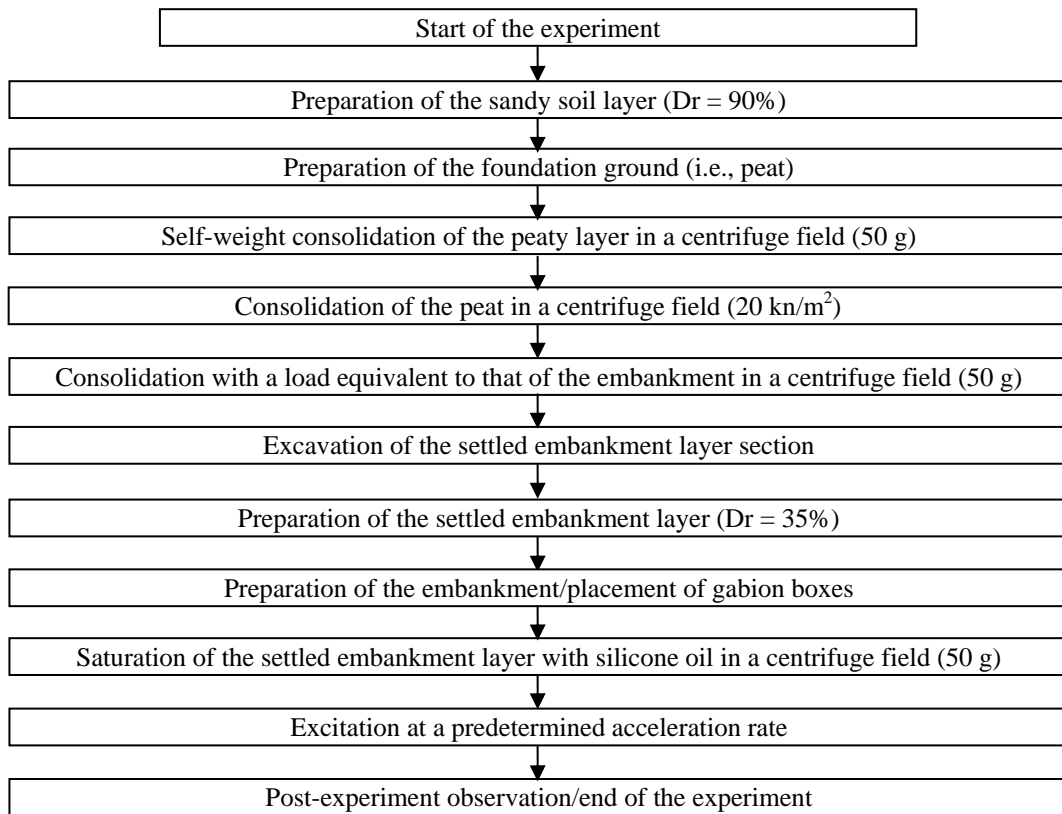


Fig. 4. Experiment procedure

Table 3. Physical properties of the peat layer

Moisture content	230 to 300%
Soil particle density	1.99 g/cm <sup>3</sup>
Compression index	3.2

Table 4. Physical properties of the peat layer

Soil particle density	2.67 g/cm <sup>3</sup>
Max. dry density	1.87 g/cm <sup>3</sup>
Opt. moisture content	9.5%
Cohesion	1.7 kN/m <sup>2</sup>
Internal friction angle	33.1°

## 4. EXPERIMENT RESULTS

### 4.1. Embankment deformation and settlement

Cases 3 and 7, which had almost the same input acceleration ( $275 \text{ m/s}^2$ ), are discussed here to highlight examples of the conditions seen after excitation. Photos 3 and 4 show these cases, respectively, and Figure 5 shows the amounts of settlement at the slope shoulder and the center of the crown.



Photo 3. Case 3 without countermeasures (input acceleration:  $275 \text{ m/s}^2$ )  
(Left: situation at the top of the embankment; right: situation as seen from the side)

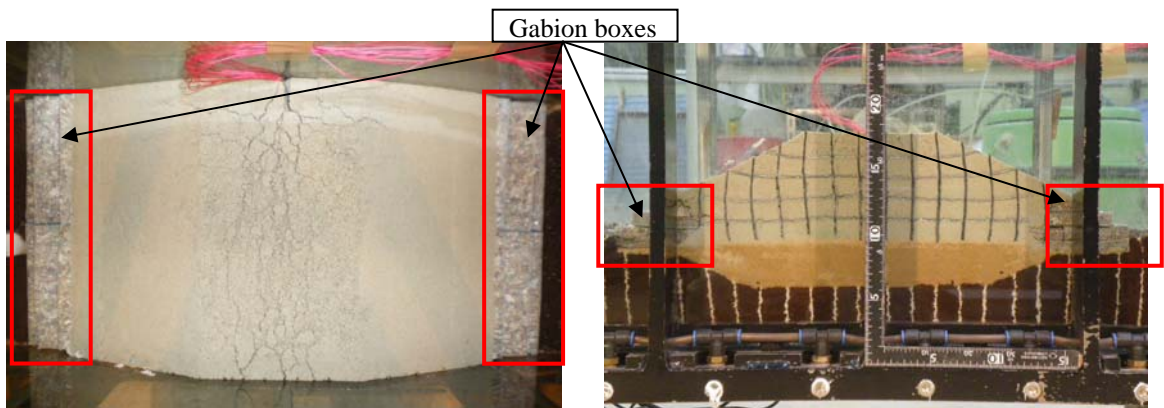


Photo 4. Case 7 with gabion boxes (input acceleration:  $275 \text{ m/s}^2$ )  
(Left: situation at the top of the embankment; right: situation seen from the side)

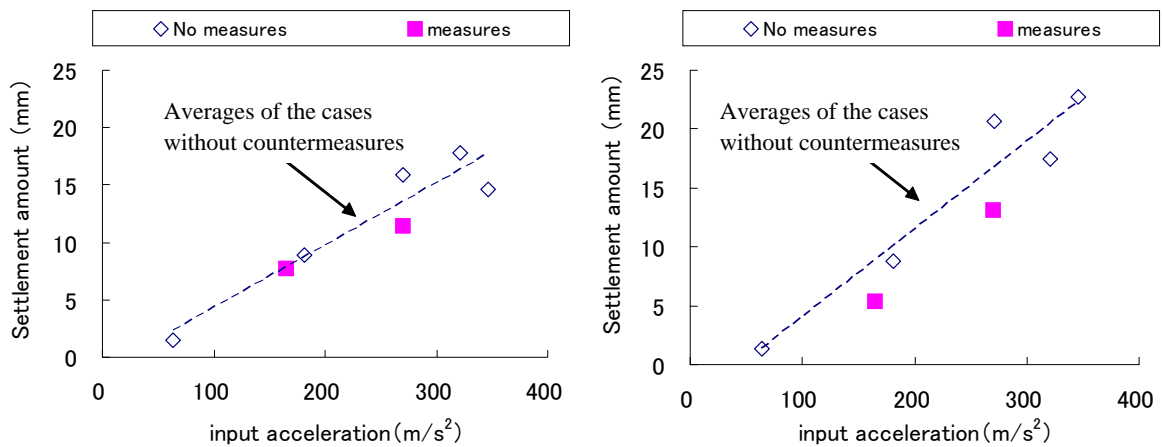


Fig. 5. Settlement in each case  
(Left: situation at the slope shoulder; right: situation at the center of the crown)

As shown in Photo 3, countless cracks were observed in the embankment crowns in Cases 3 to 5 without countermeasures and with large input acceleration. The cracks became deeper with higher levels of input acceleration. The view from the side shows that the sections near the embankment slope toe had moved considerably toward the outside. The embankments had an appearance of having been crushed, as seen with the embankment damage seen after the Great East Japan Earthquake of 2011 and the Kushiro-oki Earthquake of 1993. It was presumed that their bottom parts lost shear force and underwent significant deformation due to the generation of excess pore water pressure.

As shown in Photo 4, the number and depth of cracks were smaller in Case 7 with gabion boxes than in Case 3 without countermeasures.

From Fig. 5, it can be seen that the amount of settlement in the cases without countermeasures increased in a linear fashion with greater input acceleration. No significant settlement was observed in Case 1 with small input acceleration. In Cases 3 to 5 without countermeasures and with input acceleration exceeding  $275 \text{ m/s}^2$ , settlement as large as 15 mm (75 cm on a full scale) occurred at the slope shoulder. At the embankment crowns, settlement of 18 to 23 mm (90 to 115 cm on a full scale) was observed.

No difference was seen between settlement at the slope shoulder in Case 6 with countermeasures using gabion boxes and that of Case 2 with a similar level of input acceleration. Although the amount of settlement at the slope shoulder in Case 6 did not differ greatly from that in Case 2, it was 5 mm (25 cm on a full scale) less at the embankment crown. Settlement in Case 7 was also 5 mm (25 cm on a full scale) less at the slope shoulder and 8 mm (40 cm on a full scale) less at the crown than that in Case 3 with similar input acceleration.

#### 4.2. Excess pore water pressure ratio in the settled embankment layers

Figure 6 shows the excess pore water pressure ratio at the bottom of the slope shoulder and the bottom of the crown center in each case.

In the cases without countermeasures, the ratio increased gradually with greater input acceleration, although the rise was not significant. In Cases 3 to 5 with high input acceleration, the ratio was around 0.2 to 0.3 at the bottom of the slope shoulder or at the bottom of the embankment crown.

There was no difference between Case 6 with gabion boxes and Case 2 with similar input acceleration at either the slope shoulder or the bottom of the crown. However, the generation of excess pore water pressure was around 60% less at the bottom of the slope shoulder and the bottom of the crown in Case 7, in which gabion boxes were also used, than in Case 3 with similar input acceleration.

It was presumed that the generation of excess pore water pressure was suppressed because the use of gabion boxes improved pore water drainage.

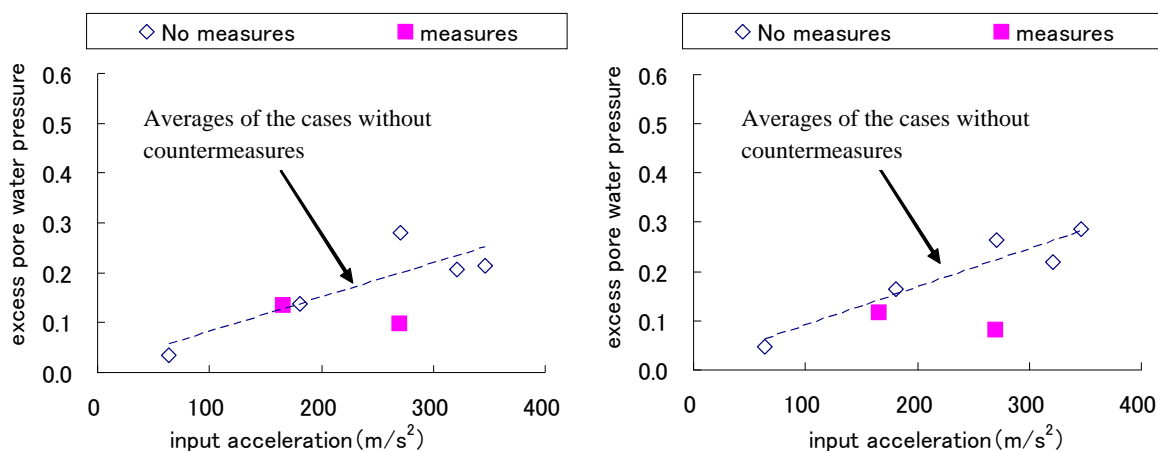


Fig. 6. Excess pore water pressure in each case  
(Left: bottom of the slope shoulder; right: bottom of the crown center)

## 5. CONCLUSION

In this study, methods for seismically reinforcing existing embankments on peaty ground against large-scale earthquakes were investigated. A centrifuge model test was conducted concerning seismic reinforcement using gabion boxes, from which settled embankment layer drainage and embankment restraint effects can be expected. The results showed that settlement was reduced by 5 to 8 mm (25 to 40 cm on a full scale) and excess pore water pressure was reduced by around 60% at the slope shoulder and embankment crown in the cases with an input acceleration of  $275 \text{ m/s}^2$ . It was inferred from these outcomes that gabion boxes were effective in improving drainage and restraining embankments.

The experiment here was limited to cases with four layers of gabion boxes, but the reinforcement effect is thought to depend on the number of layers and the depth of the boxes. Accordingly, the authors plan to study these points in future work to identify countermeasures with higher seismic reinforcement effects.

### References

- (1) Japan Institute of Construction Engineering: Advancement of Future Aseismic Measures for River Embankments Based on the Effects of the Great East Japan Earthquake (report), 2011 (in Japanese)
- (2) Civil Engineering Research Institute (CERI): Report on Investigation of Damage Caused by the Kushiro-Oki Earthquake of 1993, *Report of the Civil Engineering Research Institute*, No. 100, pp. 13 – 54, 1993 (in Japanese)
- (3) Hayashi H., Nishimoto S., Hashimoto H.: Earthquake Resistance of Embankments Constructed on Peaty Ground, Monthly Report of Civil Engineering Research Institute For Cold Region (CERI) No. 657, pp. 15 – 23, 2008 (in Japanese)
- (4) Sasaki, Y. et al.: Embankment Failure Caused by the Kushiro-Oki Earthquake of January 15, 1993, *Proc. of Performance of Ground and Soil Structures during Earthquakes*, 1993